Journal of Solid Mechanics Vol. 11, No. 3 (2019) pp. 535-549
DOI: 10.22034/JSM.2019.666851

Investigating Nonlinear Vibration Behavior of Rotors with Asymmetry Shaft Considering Misalignment

A.A. Jafari, P. Jamshidi *

Department of Mechanical Engineering, KNT University, Tehran, Iran

Received 3 June 2019; accepted 1 August 2019

ABSTRACT

In this paper, the nonlinear vibration behavior of a rotor with asymmetric shaft considering misalignment is studied. The system consists of a rectangular shaft and a disk, which is connected to a motor through a flexible coupling. In order to consider higher order deformations, nonlinear Bernoulli beam is used for modeling the shaft. Gibbons' equations are utilized to apply misaligned coupling forces. The equations of motion of the system are derived using the Lagrangian method and then discretized by the Rayleigh-Ritz method. In order to solve nonlinear equations and hence obtaining nonlinear responses, multiple scales method is used. The vibration behavior of the system near the resonance frequencies is studied by taking into account various parameters including unbalance forces and the effect of the asymmetry of cross section of the shaft. The analytical results are consistent with those of numerical method with a good accuracy. In addition, the effects of variations of the system parameters on the rotor vibration behavior have been shown graphically. In the end, the changes in the various parameters of the system and their effects on the rotor vibration response are discussed.

Keywords: Nonlinear vibration, Rotor dynamics, Asymmetric shaft, Misalignment.

1 INTRODUCTION

THE dynamic behavior of rotors is one of the significant fields in which extensive researches have been carried out so far. The focus of these works has been on shafts with a circular cross-section while in industry; there are rotary machines such as generators, electro motors or some of their components including couplings and screw shafts that are not symmetric. Regarding misalignment of rotors, due to its importance and its effects on vibrations, various studies have been done. However, the effects of misalignment on asymmetric rotors have rarely been investigated yet. In the case of the consequences of asymmetric rotors, Tondl [1] analyzed the effects of the variability of shaft stiffness on the vibration behavior of the system and then determined the boundaries of instability. Badlani [2] also examined the stability of the asymmetric rotor with a more precise model. He found new boundaries of instability, taking into account the theory of Timoshenko's beam. Sheu [3] studied the results of

*Corresponding author. Tel.: +98 021 22850595; Fax.:+98 021 44908705.
E-mail address: pouya.jamshidi@mail.kntu.ac.ir (P. Jamshidi).

harmonic forces as well as dynamic forces on instability boundaries. Pei [4] also studied the boundaries of instability of a rotor with parametric excitation. He showed that the boundaries of instability are beyond the boundaries of instability obtained by Floquet method. Shahgholi [5] also acquired the main and parametric resonances of an asymmetric rotor considering the nonlinear effects due to higher order deformations. He applied multiple scales method to solve motion equations and showed the rotor's vibration behavior as well as unstable boundaries near the resonances. Jafari [6] solved the nonlinear motion equations for an asymmetric rotor using a perturbation method and using higher terms led to stability boundaries. He demonstrated that semi-analytic methods have more accuracy in solving nonlinear shafts with asymmetric sections when nonlinear terms are small. Gibbons [7] stated that the lack of alignment causes coupling forces and moments, which are the main reasons of vibrations in rotating machines. He calculated the forces and moments for various couplings and presented in his article. Sekhar et al. [8] developed Gibbons' model. They considered 8 degrees of freedom for each node (4 degrees for each plane) to determine displacement, slope, shear force and bending moment for each node. They assumed that the misalignment causes excitation force at a frequency twice the rotational speed (i.e. 2X). Al-Hussain et al. [9] examined the effect of the misalignment due to the parallel misalignment in the dynamic response of the rotor. They first obtained the motion equations for the proposed model based on the energy method. They concluded that parallel misalignment would only affect vibrations in a steady-state equilibrium frequency, and higher harmonic vibrations are caused by nonlinear effects of the system and the asymmetry of bearings and rotors. A year later, in another article [10], he developed his model and added the bearing effect to his model using the Lyapunov method, examining the stability of the rotor in the presence of effects of angular misalignment. Lees [11] investigated misalignment in a rigid coupling rotor. He argued in his article that even without the nonlinear properties of a lubricant film in bearings or without considering the effects of flexible couplings, the vibrations caused by the misalignment can be observed at 2X harmonic. Patel and his colleague [12] and [13] performed a combination of theoretical and laboratory work to acquire more precise results on the study of the effects of misalignment on the frequency response of the rotor. In their model, they utilized finite element method taking into account Timoshenko beam with 6 degrees of freedom and modeling misalignment as a force vector at the point in the coupling location obtained using laboratory data. Pennacchi [14] examined the misalignment impacts on a more complex model. His model was similar to the real turbo generator. They also considered bearing effects in their model and solved the problem using finite element method. Similar to the other researchers, they observed the super-harmonic vibrations as a result of non-linear effects of rotor components including bearings. Ma [15] scrutinized the bearing's instability due to rotor misalignment. They used the proposed Gibbons' model to study the misalignment. They solved the problem using finite element method and taking into account the Timoshenko beam element with four degrees of freedom in each node as well as considering the gyroscopic effect of disks.

In the case of rotor vibrations with an asymmetry section, considering misalignment, rarely research has been done, and only the work of Sheng [16] in 2012 has been mentioned. The model of their study included two axes and a flexible coupling, each with a disk and one of the axes having asymmetric section. Using the Lagrangian method, they extracted the equations and used numerical methods. In their model, they examined only the effect of parallel misalignment. They showed that parallel misalignment and unbalance mass in shafts with asymmetry section increase the amount of vibration amplitude at the natural frequency of the system while the variable stiffness of shaft increases the amount of vibration amplitude at a frequency equal to half the system natural frequency.

This research intends to analyze analytically and numerically the nonlinear vibration behavior of a rotor in which shafts with rectangular section are used under coupling forces due to misalignment. The moment of inertia of rotary parts, the gyroscopic effect, the effects of higher order nonlinear displacements in the strain energy of shaft and the affects of unbalance force are considered. The changes in the moment of inertia are also taken into account as well as the shaft stiffness variations in rotor rotational motion. Using the angles of Euler, the kinetic energy of the rotor is calculated and applying the theory of nonlinear Bernoulli beam, strain energy of rotor is derived. The Lagrange method is utilized to extract the motion equations and these coupled equations are solved by the multiple scales method.

2 FORMULATION AND MOTION EQUATIONS

In this study, the model includes a single rectangular-section shaft with a disk mounted on which are connected to an electric motor through a coupling. The model is shown in Fig.1. The shaft is a beam with rectangular cross section and length L. The disk is assumed rigid with radius R. Unbalance mass of disk is denoted by $m_{unbalance}$ .The

displacement components in the *x, y*, and *z* directions are represented by $u(x,t), v(x,t)$ and $w(x,t)$ respectively as shown in Fig.2.

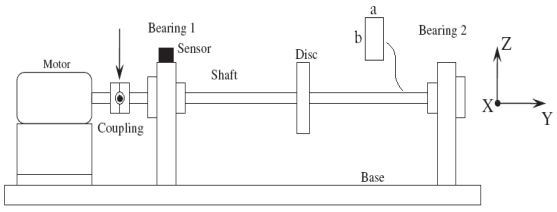

Fig.1
Rotor system coupled with electric motor.

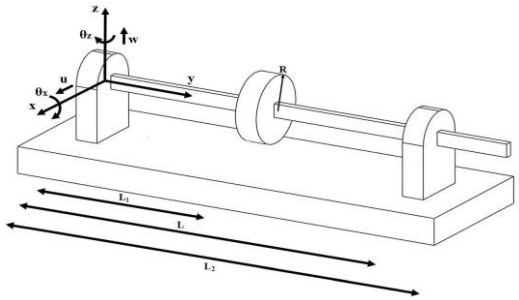

Fig.2
Rotor system using shaft with rectangular cross section.

The kinetic energy of the disk can be derived as follows:

$$T_D = \frac{1}{2} M_D (\dot{u}^2 + \dot{w}^2) + \frac{1}{2} (I_{Dx} \omega_x^{\ 2} + I_{Dy} \omega_y^{\ 2} + I_{Dz} \omega_z^{\ 2}) \tag{1}$$

where M_D, I_{Dx}, I_{Dy} and I_{Dz} are mass of disk and moment inertia of disk about principal directions. ω_x, ω_y and ω_z are rotational speeds of disk, which are extracted as below:

$$\omega_x = -\dot{\theta}_z \cos\theta_x \sin\phi + \dot{\theta}_x \cos\phi,\ \omega_y = \dot{\phi} + \dot{\theta}_z \sin\theta_x,\quad \omega_z = \dot{\theta}_z \cos\theta_x \cos\phi + \dot{\theta}_x \sin\phi \tag{2}$$

where θ_z, θ_x and ϕ are Euler angles [17]. Since torsion deformations are neglected and rotational speed of rotor is constant, the magnitude of $\dot{\phi}$ is equal to that of Ω.

The kinetic energy of shaft with rectangular section and the kinetic energy due to mass unbalance denoted by T_s and T_u respectively. Referring to [17], they are calculated as follows:

$$T_s = \frac{1}{2}\rho A \int_0^L (\dot{u}^2 + \dot{w}^2) dy + \frac{1}{2}\rho I \int_0^L (\dot{\theta}_x^{\ 2} + \dot{\theta}_z^{\ 2} + 4\Omega \dot{\theta}_z \theta_x) dy + \frac{1}{2}\rho \Delta I \int_0^L (\cos 2\Omega t (\dot{\theta}_x^{\ 2} - \dot{\theta}_z^{\ 2}) - 2\dot{\theta}_z \dot{\theta}_x \sin 2\Omega t)\, dy \tag{3}$$

$$T_u = m_{unbalance} \Omega d (\dot{u} \cos\Omega t - \dot{w} \sin\Omega t) \tag{4}$$

Therefore, the total kinetic energy of rotor T_R, using the Eqs. (1), (3) and (4) can be obtained as:

$$\begin{aligned} T_R = {} & \frac{1}{2}\rho A \int_0^L (\dot{u}^2 + \dot{w}^2) dy + \frac{1}{2}\rho I \int_0^L (\dot{\theta}_x^{\ 2} + \dot{\theta}_z^{\ 2} + 4\Omega \dot{\theta}_z \theta_x) dy + \frac{1}{2}\rho \Delta I \int_0^L (\cos 2\Omega t (\dot{\theta}_x^{\ 2} - \dot{\theta}_z^{\ 2}) - 2\dot{\theta}_z \dot{\theta}_x \sin 2\Omega t)\, dy + \frac{1}{2} M_D (\dot{u}^2 + \dot{w}^2) \\ & + \frac{1}{2} I_{Dx} (\dot{\theta}_x^{\ 2} + \dot{\theta}_z^{\ 2}) + I_{Dy} (\Omega \dot{\theta}_z \theta_x) + m_{unbalance} \Omega d (\dot{u} \cos\Omega t - \dot{w} \sin\Omega t) \end{aligned} \tag{5}$$

where $I = \frac{I_x - I_z}{2}$, $\Delta I = \frac{I_x - I_z}{2}$ and I_x and I_z are moment inertias about *x* and *z* respectively.

The strain energy of shaft with rectangular section and taking into account higher order deformations are obtained in the form of following equations [17]:

$$U_s = \frac{EI}{2}\int_0^L [(\frac{\partial^2 u}{\partial y^2})^2 + (\frac{\partial^2 w}{\partial y^2})^2]dy + \frac{E\Delta I}{2}\int_0^L [((\frac{\partial^2 w}{\partial y^2})^2 - (\frac{\partial^2 u}{\partial y^2})^2)(\cos^2 \Omega t - \sin^2 \Omega t) + 4(\frac{\partial^2 u}{\partial y^2})(\frac{\partial^2 w}{\partial y^2})\sin \Omega t \cos \Omega t]dy$$
$$+ \frac{EA}{8}\int_0^L [((\frac{\partial u}{\partial y})^2 + (\frac{\partial w}{\partial y})^2)^2]dy \tag{6}$$

According to $\theta_x = \frac{\partial w}{\partial y}, \theta_z = -\frac{\partial u}{\partial y}$ the Eq. (6) can be rewritten as follows:

$$U_s = \frac{EI}{2}\int_0^L [(\frac{\partial \theta_z}{\partial y})^2 + (\frac{\partial \theta_x}{\partial y})^2]dy + \frac{E\Delta I}{2}\int_0^L [((\frac{\partial \theta_x}{\partial y})^2 - (\frac{\partial \theta_z}{\partial y})^2)\cos 2\Omega t - 2(\frac{\partial \theta_z}{\partial y})(\frac{\partial \theta_x}{\partial y})\sin 2\Omega t]dy + \frac{EA}{8}\int_0^L [(\theta_z^2 + \theta_x^2)^2]dy \tag{7}$$

In this research, Gibbons' reaction forces [7] are the static load for stationary rotors. For a rotating shaft, the forces act as a periodic load with a function of half-sinusoidal, having time period of π/Ω. In order to analyze the effect of misaligned coupling forces in both first and second rotational speed, 1X and 2X components are considered and in this paper, theoretical model based on Gibbon and Ref. [18] is assumed as follows:

$$F_{mis1} = f_1 \sin \Omega t + f_1 \sin 2\Omega t, \quad F_{mis2} = f_2 \cos \Omega t + f_2 \cos 2\Omega t \tag{8}$$

where f_1 and f_2 are obtained according to Gibbons' equations. (Appendix A2)

3 USING THE RAYLEIGH - RITZ METHOD

For approximation of the functions *u* and *w*, displacements in *x* and *z* directions, the Rayleigh-Ritz method can be used. In this method, the values *u* and *w* can be expressed in the form of the following equation.

$$u(y,t) = f(y)q_1(t)\ , w(y,t) = f(y)q_2(t) \tag{9}$$

and the angular displacements and derivatives are expressed in the following form:

$$\theta_x = \frac{\partial w}{\partial y} = \frac{df(y)}{dy}q_2(t) = g(y)q_2(t)\ , \theta_z = -\frac{\partial u}{\partial y} = -\frac{df(y)}{dy}q_1(t) = -g(y)q_1(t)$$
$$\frac{\partial^2 u}{\partial y^2} = \frac{d^2 f(y)}{dy^2}q_1(t) = h(y)q_1(t), \ \frac{\partial^2 w}{\partial y^2} = \frac{d^2 f(y)}{dy^2}q_2(t) = h(y)q_2(t) \tag{10}$$

where derivatives are defined with respect to y. Substituting the Eqs. (9) and (10) in (5), the kinetic and strain energy of the rotor are obtained in the form of:

$$T_R = \frac{1}{2}a_1(\dot{q}_1^{\,2} + \dot{q}_2^{\,2}) - a_2\Omega\dot{q}_1 q_2 + m_{unbalance}\Omega df(l_1)(\dot{q}_1 \cos \Omega t - \dot{q}_2\, sin\Omega t) + \frac{1}{2}a_3(\dot{q}_2^{\,2} - \dot{q}_1^{\,2})\cos 2\Omega t + a_3\dot{q}_1\dot{q}_2 \sin 2\Omega t \tag{11}$$

where

$$\begin{cases} a_1 = \rho A\int_0^L f(y)^2 dy + \rho I\int_0^L g(y)^2 dy + M_D f(l_1)^2 + I_{Dx} g(l_1)^2 \\ a_2 = 2\rho I\int_0^L g(y)^2 dy + I_{Dy}\Omega g(l_1)^2 \, , a_3 = \rho\Delta I\int_0^L g(y)^2 dy \end{cases} \tag{12}$$

$$U_s = \frac{b_1}{2}(q_1^{\,2}(t) + q_2^{\,2}(t)) + \frac{b_2}{2}(q_2^{\,2}(t) - q_1^{\,2}(t))\cos 2\Omega t + b_2 q_1(t) q_2(t)\sin 2\Omega t + \frac{b_3}{8}(q_1^{\,2}(t) + q_2^{\,2}(t))^2 \tag{13}$$

where

$$b_1 = EI\int_0^L h^2(y)dy,\ b_2 = E\Delta I\int_0^L h^2(y)dy, b_3 = EA\int_0^L g^4(y)dy \tag{14}$$

The Lagrange method is used to derive the motion equations. Lagrange equations for a *k*-degree system can be given as:

$$\begin{aligned} &L = T - U \\ &\frac{d}{dt}(\frac{\partial L}{\partial \dot{q}_k}) - \frac{\partial L}{\partial q_k} = Q_k \end{aligned} \tag{15}$$

In the above equation, L is Lagrange and is equal to the difference between kinetic and strain energies. q_k is general characteristics and Q_k is general force corresponding to it.

In this paper, the forces due to misaligned coupling assumed as external forces applied on the coupling at a distance L_2 from the bearing No.2. Using Eq. (9) , the following equation can be derived:

$$\begin{aligned} &\delta W = F_{mis1} f(L_2)\sin\Omega t\delta q_1 + F_{mis1} f(L_2)\sin 2\Omega t\delta q_1 \\ &F_{mis2} f(L_2)\cos\Omega t\delta q_2 + F_{mis2} f(L_2)\cos 2\Omega t\delta q_2 \end{aligned} \tag{16}$$

So, Q_1 and Q_2 are the general forces due to misaligned coupling in the direction *x* and *z*, respectively, and are computed as [17]:

$$Q_1 = F_{mis1} f(L_2)\sin\Omega t + F_{mis1} f(L_2)\sin 2\Omega t \tag{17}$$

$$Q_2 = F_{mis2} f(L_2)\cos\Omega t + F_{mis2} f(L_2)\cos 2\Omega t \tag{18}$$

By applying Lagrange's method and taking into account the damping forces, the unbalance mass and the force generated by the misalignment, the motion equations can be derived as:

$$\begin{aligned} &\ddot{q}_1 - \lambda_1\Omega\dot{q}_2 + \beta_1 q_1 + \frac{\beta_3}{2}(q_1^{\,2} + q_2^{\,2})q_1 - \lambda_2\ddot{q}_1\cos 2\Omega t + \lambda_2\dot{q}_1(2\Omega)\sin 2\Omega t + \lambda_2\ddot{q}_2\sin 2\Omega t + \lambda_2\dot{q}_2(2\Omega)\cos 2\Omega t \\ &-\beta_2 q_1\cos 2\Omega t + \beta_2 q_2\sin 2\Omega t + c\dot{q}_1 = [m_e\Omega^2 df(l_1) + f_{mis1} f(L_2)]\sin\Omega t + f_{mis1} f(L_2)\sin 2\Omega t \end{aligned} \tag{19}$$

$$\begin{aligned} &\ddot{q}_2 + \lambda_1\Omega\dot{q}_1 + \beta_1 q_2 + \frac{\beta_3}{2}(q_1^{\,2} + q_2^{\,2})q_2 + \lambda_2\ddot{q}_2\cos 2\Omega t - \lambda_2\dot{q}_2(2\Omega)\sin 2\Omega t + \lambda_2\ddot{q}_1\sin 2\Omega t + \lambda_2\dot{q}_1(2\Omega)\cos 2\Omega t \\ &+\beta_2 q_2\cos 2\Omega t + \beta_2 q_1\sin 2\Omega t + c\dot{q}_2 = [m_e\Omega^2 df(l_1) + f_{mis2} f(L_2)]\cos\Omega t + f_{mis2} f(L_2)\cos 2\Omega t \end{aligned} \tag{20}$$

where *c* is damping coefficient and,

$$\lambda_1 = \frac{a_2}{a_1}, \lambda_2 = \frac{a_3}{a_1}, \beta_1 = \frac{b_1}{a_1},\ \beta_2 = \frac{b_2}{a_1}, \beta_3 = \frac{b_3}{a_1}, \beta_0 = \frac{b_0}{a_1}, m_e = \frac{m_{unbalance}}{a_1}, f_{mis1} = \frac{F_{mis1}}{a_1}, f_{mis2} = \frac{F_{mis2}}{a_1} \tag{21}$$

4 SOLVING THE MOTION EQUATIONS

In this section, in order to solve ordinary differential equations i.e. the Eqs. (14) and (15), multiple scales method is used. This method is very effective in solving nonlinear equations. To apply this method, the displacement in the transverse directions of the shaft x and z are expanded, respectively, as follows:

$$\begin{aligned} q_1(T_0,T_1) &= q_{10}(T_0,T_1) + q_{11}(T_0,T_1)\varepsilon + ... \\ q_2(T_0,T_1) &= q_{20}(T_0,T_1) + q_{21}(T_0,T_1)\varepsilon + ... \end{aligned} \tag{22}$$

where $T_0 = t$ and $T_1 = \varepsilon t$ are respectively fast and slow time scale and ε is a small non-dimensional parameter. In order to solve the Eqs. (19) and (20), the nonlinear term due to high order deformation (β_3) and coefficients λ_2 , β_2 related to stiffness variation in Mathieu's equation and also damping and forcing terms are assumed small so that they appear in the ε order. Therefore parametric values $c\varepsilon$, $\lambda_2\varepsilon$, $\beta_2\varepsilon$, $\beta_3\varepsilon$, $m_e\varepsilon$, $f_{mis1}\varepsilon$ and $f_{mis2}\varepsilon$ are substituted by c , λ_2 , β_2 , β_3 , m_e , f_{mis1} and f_{mis2} in Eqs. (19) and (20).

$$\begin{aligned} &\ddot{q}_1 - \lambda_1\Omega\dot{q}_2 + \beta_1 q_1 + \frac{\beta_3}{2}(q_1^{\,2} + q_2^{\,2})q_1\varepsilon - \lambda_2\ddot{q}_1\cos 2\Omega t\varepsilon + \lambda_2\dot{q}_1(2\Omega)\sin 2\Omega t\varepsilon + \lambda_2\ddot{q}_2\sin 2\Omega t\,\varepsilon + \lambda_2\dot{q}_2(2\Omega)\cos 2\Omega t\varepsilon \\ &-\beta_2 q_1\cos 2\Omega t\varepsilon + \beta_2 q_2\sin 2\Omega t\varepsilon + c\dot{q}_1\,\varepsilon = [m_e\Omega^2 df(l_1) + f_{mis1}f(L_2)]\sin\Omega t\,\varepsilon + f_{mis1}f(L_2)\sin 2\Omega t\,\varepsilon \end{aligned} \tag{23}$$

$$\begin{aligned} &\ddot{q}_2 + \lambda_1\Omega\dot{q}_1 + \beta_1 q_2 + \frac{\beta_3}{2}(q_1^{\,2} + q_2^{\,2})q_2\,\varepsilon + \lambda_2\ddot{q}_2\cos 2\Omega t\varepsilon - \lambda_2\dot{q}_2(2\Omega)\sin 2\Omega t\varepsilon + \lambda_2\ddot{q}_1\sin 2\Omega t\varepsilon + \lambda_2\dot{q}_1(2\Omega)\cos 2\Omega t\varepsilon \\ &+\beta_2 q_2\cos 2\Omega t\varepsilon + \beta_2 q_1\sin 2\Omega t\varepsilon + c\dot{q}_2\,\varepsilon = [m_e\Omega^2 df(l_1) + f_{mis2}f(L_2)]\cos\Omega t\,\varepsilon + f_{mis2}f(L_2)\cos 2\Omega t\,\varepsilon \end{aligned} \tag{24}$$

Substituting Eq. (22) into equations Eqs. (23) and (24) and Equalizing the terms of the same order, the following equations are obtained:

$$\begin{aligned} &\varepsilon^0: \\ &\ddot{q}_{10} - \lambda_1\Omega\dot{q}_{20} + \beta_1 q_{10} = 0 \\ &\ddot{q}_{20} + \lambda_1\Omega\dot{q}_{10} + \beta_1 q_{20} = 0 \end{aligned} \tag{25}$$

$$\begin{aligned} &\varepsilon^1: \\ &D_0^{\,2}q_{11} - \lambda_1\Omega(D_0q_{21}) + \beta_1 q_{11} = -2D_0D_1q_{10} + \lambda_1\Omega D_1q_{20} - \frac{\beta_3}{2}((q_{10}^{\,2} + q_{20}^{\,2})q_{10} + \lambda_2 D_0^{\,2}q_{10}\cos 2\Omega t - \lambda_2 D_0q_{10}(2\Omega)\sin 2\Omega t - \lambda_2 D_0^{\,2}q_{20}\sin 2\Omega t \\ &-\lambda_2 D_0q_{20}2\Omega\cos 2\Omega t + \beta_2 q_{10}\cos 2\Omega t - \beta_2 q_{20}\sin 2\Omega t - cDq_{10} + [m_e\Omega^2 df(l_1) + f_{mis1}f(L_2)]\sin\Omega t + f_{mis1}f(L_2)\sin 2\Omega t \end{aligned} \tag{26}$$

$$\begin{aligned} &D_0^{\,2}q_{21} + \lambda_1\Omega D_0q_{11} + \beta_1 q_{21} = -2D_0D_1q_{20} - \lambda_1\Omega D_1q_{10} - \frac{\beta_3}{2}(q_{10}^{\,2} + q_{20}^{\,2})q_{20} - \lambda_2 D_0^{\,2}q_{20}\cos 2\Omega t + \lambda_2 D_0q_{20}(2\Omega)\sin 2\Omega t \\ &-\lambda_2 D_0^{\,2}q_{10}\sin 2\Omega t - \lambda_2 D_0q_{10}(2\Omega)\cos 2\Omega t - \beta_2 q_{20}\cos 2\Omega t - \beta_2 q_{10}\sin 2\Omega t - c\,D_0q_{20} + [m_e\Omega^2 df(l_1) + f_{mis2}f(L_2)]\cos\Omega t \\ &+f_{mis2}f(L_2)\cos 2\Omega t \end{aligned} \tag{27}$$

The solution of Eqs. (25) will be in the form of:

$$q_{10} = A_1(T_1)\exp(i\omega_1T_0) + A_2(T_1)\exp(i\omega_2T_0) + cc \tag{28}$$

$$q_{20} = \Lambda_1A_1\exp(i\omega_1T_0) + \Lambda_2A_2\exp(i\omega_2T_0) + cc \tag{29}$$

where

$$\Lambda_1 = \frac{i(\omega_1^2 - \beta_1)}{\lambda_1 \omega_1 \Omega}\ , \quad \Lambda_2 = \frac{i(\omega_2^2 - \beta_1)}{\lambda_1 \omega_2 \Omega} \tag{30}$$

The two resonance frequencies ω_1 and ω_2 are the primary resonance frequencies, which are the solution of the following equation:

$$\omega^4 - (2*\beta_1 + \lambda_1^2\Omega^2)\omega^2 + \beta_1^2 = 0 \tag{31}$$

Substituting Eqs. (28) and (29) into Eqs. (26) and (27) and then Simplifying them, following equations will be derived:

$$\begin{aligned}
&D_0^2 q_{11} - \lambda_1\Omega(D_0 q_{21}) + \beta_1 q_{11} = -\frac{\beta_3}{2}[(1+\Lambda_1^2)A_1^3 \exp[3i\omega_1 T_0] + (3+\Lambda_2^2+2\Lambda_1\Lambda_2)A_1 A_2^2 \exp[i(\omega_1+2\omega_2)T_0] \\
&+(3+\Lambda_1^2+2\Lambda_1\Lambda_2)A_1^2 A_2 \exp[i(2\omega_1+\omega_2)T_0] + [-2i\omega_1 D_1 A_1(T_1) + \lambda_1\Omega\Lambda_1 D_1 A_1 + (3+\Lambda_1\overline{\Lambda}_2+\Lambda_1\overline{\Lambda}_1+\Lambda_1^2)A_1^2\overline{A}_1 \\
&+(6+2\Lambda_2\overline{\Lambda}_2+2\Lambda_1\overline{\Lambda}_2+\Lambda_1\Lambda_2)A_1 A_2\overline{A}_2 - ic\omega_1 A_1]\exp[i\omega_1 T_0] + [-2i\omega_2 D_1 A_2(T_1) + \Lambda_2\lambda_1\Omega D_1 A_2 \\
&+(6+2\overline{\Lambda}_1\Lambda_2+2\Lambda_1\overline{\Lambda}_1+2\Lambda_1\Lambda_2)A_1\overline{A}_1 A_2 + (3+2\Lambda_2\overline{\Lambda}_2+\Lambda_2^2)A_2^2\overline{A}_2 - ic\omega_2 A_2]\exp[i\omega_2 T_0] + \\
&(1+\overline{\Lambda}_2^2)A_1\overline{A}_2^2 \exp[i(\omega_1-2\omega_2)T_0] + (2+2\Lambda_1\overline{\Lambda}_2)A_1^2\overline{A}_2 \exp[i(2\omega_1-\omega_2)T_0] + (1+\Lambda_2^2)A_2^3 \exp[3i\omega_2 T_0] \\
&+(2+2\overline{\Lambda}_1\Lambda_2)\overline{A}_1 A_2^2 \exp[i(2\omega_2-\omega_1)T_0] + (1+\overline{\Lambda}_1^2)\overline{A}_1^2 A_2[i(\omega_2-2\omega_1)T_0] + cc] - \frac{1}{2}i[m_e\Omega^2 df(l_1) \\
&+f_{mis1} f(L_2)]\exp(i\Omega T_0) - \frac{1}{2}if_{mis1} f(L_2)\exp(i2\Omega T_0) + cc \\
&\frac{1}{2}[-\lambda_2\omega_1^2 - \lambda_2\omega_1(2\Omega) - \lambda_2 i\omega_1^2\Lambda_1 - \lambda_2\omega_1\Lambda_1 i(2\Omega) + \beta_2 + \beta_2 i\Lambda_1]A_1 \exp[i(2\Omega+\omega_1)] \\
&\frac{1}{2}[-\lambda_2\omega_1^2 + \lambda_2\omega_1(2\Omega) + \lambda_2 i\omega_1^2\Lambda_1 - \lambda_2\omega_1\Lambda_1 i(2\Omega) + \beta_2 - \beta_2 i\Lambda_1]\overline{A}_1 \exp[i(2\Omega-\omega_1)] \\
&\frac{1}{2}[-\lambda_2\omega_2^2 - \lambda_2\omega_2(2\Omega) - \lambda_2 i\omega_2^2\Lambda_2 - \lambda_2\omega_2\Lambda_2 i(2\Omega) + \beta_2 + \beta_2 i\Lambda_2]A_2 \exp[i(2\Omega+\omega_2)] \\
&\frac{1}{2}[-\lambda_2\omega_2^2 + \lambda_2\omega_2(2\Omega) + \lambda_2 i\omega_2^2\Lambda_2 - \lambda_2\omega_2\Lambda_2 i(2\Omega) + \beta_2 - \beta_2 i\Lambda_2]\overline{A}_2 \exp[i(2\Omega-\omega_2)]
\end{aligned} \tag{32}$$

$$\begin{aligned}
&D_0^2 q_{21} + \lambda_1\Omega D_0 q_{11} + \beta_1 q_{21} = -\frac{\beta_3}{2}[(\Lambda_1+\Lambda_1^3)A_1^3 \exp[3i\omega_1 T_0] + (\Lambda_1+2\Lambda_2+3\Lambda_1\Lambda_2^2)A_1 A_2^2 \exp[i(\omega_1+2\omega_2)T_0] + \\
&(2\Lambda_1+\Lambda_2+3\Lambda_1^2\Lambda_2)A_1^2 A_2 \exp[i(2\omega_1+\omega_2)T_0] + [-2\Lambda_1 i\omega_1 D_1 A_1 - \lambda_1\Omega D_1 A_1(T_1) + (2\Lambda_1+\overline{\Lambda}_1+3\Lambda_1^2\overline{\Lambda}_1)A_1^2\overline{A}_1 \\
&+(2\Lambda_1+2\Lambda_2+2\overline{\Lambda}_2+6\Lambda_1\Lambda_2\overline{\Lambda}_2)A_1 A_2\overline{A}_2 - ic\omega_1\Lambda_1 A_1]\exp[i\omega_1 T_0] + \\
&[-2\Lambda_2 i\omega_1 D_1 A_2 - \lambda_1\Omega D_1 A_2(T_1) + (2\Lambda_1+2\Lambda_2+2\overline{\Lambda}_1+6\Lambda_1\overline{\Lambda}_1\Lambda_2)A_1\overline{A}_1 A_2 + (2\Lambda_2+\overline{\Lambda}_2+3\Lambda_2^2\overline{\Lambda}_2)A_2^2\overline{A}_2 - ic\omega_2\Lambda_2 A_2]\exp[i\omega_2 T_0] + \\
&+(\Lambda_1+2\overline{\Lambda}_2+3\Lambda_1\overline{\Lambda}_2^2)A_1\overline{A}_2^2 \exp[i(\omega_1-2\omega_2)T_0] + (2\Lambda_1+\overline{\Lambda}_2+3\Lambda_1^2\overline{\Lambda}_2)A_1^2\overline{A}_2 \exp[i(2\omega_1-\omega_2)T_0] + \\
&(\Lambda_2+\Lambda_2^3)A_2^3 \exp[3i\omega_2 T_0] + cc\ ] + \frac{1}{2}[m_e\Omega^2 df(l_1) + f_{mis2} f(L_2)]\exp(i\Omega T_0) + \frac{1}{2}f_{mis2} f(L_2)\exp(i2\Omega T_0) + cc \\
&\frac{1}{2}[\lambda_2\omega_1^2\Lambda_1 + \lambda_2\omega_1\Lambda_1(2\Omega) - \lambda_2 i\omega_1^2 - \lambda_2 i\omega_1(2\Omega) + \beta_2 i - \beta_2\Lambda_1]A_1 \exp[i(2\Omega+\omega_1)] \\
&\frac{1}{2}[-\lambda_2\omega_1^2\Lambda_1 + \lambda_2\omega_1\Lambda_1(2\Omega) - \lambda_2 i\omega_1^2 + \lambda_2 i\omega_1(2\Omega) + \beta_2 i + \beta_2\Lambda_1]\overline{A}_1 \exp[i(2\Omega-\omega_1)] \\
&\frac{1}{2}[\lambda_2\omega_2^2\Lambda_2 + \lambda_2\omega_2\Lambda_2(2\Omega) - \lambda_2 i\omega_2^2 + \lambda_2 i\omega_2(2\Omega) + \beta_2 i - \beta_2\Lambda_2]A_2 \exp[i(2\Omega+\omega_2)] \\
&\frac{1}{2}[-\lambda_2\omega_2^2\Lambda_2 + \lambda_2\omega_2\Lambda_2(2\Omega) - \lambda_2 i\omega_2^2 + \lambda_2 i\omega_2(2\Omega) + \beta_2 i + \beta_2\Lambda_2]\overline{A}_2 \exp[i(2\Omega-\omega_2)]
\end{aligned} \tag{33}$$

Since Eqs. (32) and (33) are linear, one can obtain a particular solution for each right term independently. To determine solvability conditions, the coefficients $\exp(i\omega_n T_0)$ of the particular solution are considered as follows: [19]

$$q_{11} = P_1(T_1)\exp(i\omega_1 T_0) + Q_1(T_1)\exp(i\omega_2 T_0)$$
$$q_{21} = P_2(T_1)\exp(i\omega_1 T_0) + Q_2(T_1)\exp(i\omega_2 T_0) \tag{34}$$

In the case Ω is near the first resonance system i.e. ω_1:

To investigate the dynamic behavior of the system near the first resonance Ω is considered in the following form:

$$\Omega = \omega_1 + \varepsilon\sigma \tag{35}$$

where σ is the detuning parameter to determine the proximity of Ω and ω_1.

Eqs. (32) and (33) will have solutions just when solvability conditions are met. To study the solvability conditions, the particular solution of the Eq. (34) by taking into account $\Omega = \omega_1 + \varepsilon\sigma$ is substituted in Eqs.(32) and (33), and the coefficients of terms of the same order are equalized [19]. By doing so, the following equations are obtained:

$$\begin{cases} (\beta_1 - \omega_1^2)P_1 - i\Omega\omega_1\lambda_1 P_2 = R_1 \\ +i\Omega\omega_1\lambda_1 P_1 + (\beta_1 - \omega_1^2)P_2 = R_2 \end{cases} \tag{36}$$

where

$$\begin{aligned} R_1 &= -2i\omega_1 D_1 A_1(T_1) + \lambda_1\Omega\Lambda_1 D_1 A_1 - \frac{\beta_3}{2}(3 + 2\Lambda_1\bar{\Lambda}_1 + \Lambda_1^2)A_1^2\bar{A}_1 - \frac{\beta_3}{2}(6 + 2\Lambda_2\bar{\Lambda}_2 + 2\Lambda_1\bar{\Lambda}_2 + 2\Lambda_1\Lambda_2)A_1A_2\bar{A}_2 \\ &-ic\omega_1 A_1 - \frac{1}{2}i[m_e\omega_1^2 df(l_1) + f_{mis1}f(L_2)]\exp(i\sigma T_1) + \frac{1}{2}[-\lambda_2\omega_1^2 + \lambda_2\omega_1(2\Omega) + \lambda_2 i\omega_1^2\Lambda_1 - \lambda_2\omega_1\Lambda_1 i(2\Omega) + \beta_2 - \beta_2 i\Lambda_1]\bar{A}_1\exp(2i\sigma T_1) \\ R_2 &= -2\Lambda_1 i\omega_1 D_1 A_1 - \lambda_1\Omega D_1 A_1(T_1) - \frac{\beta_3}{2}(2\Lambda_1 + \bar{\Lambda}_1 + 3\Lambda_1^2\bar{\Lambda}_1)A_1^2\bar{A}_1 \\ &-\frac{\beta_3}{2}(2\Lambda_1 + 2\Lambda_2 + 2\bar{\Lambda}_2 + 6\Lambda_1\Lambda_2\bar{\Lambda}_2)A_1A_2\bar{A}_2 - ic\omega_1\Lambda_1 A_1 + \frac{1}{2}[m_e\omega_1^2 df(l_1) + f_{mis2}f(L_2)]\exp(i\sigma T_1) \\ &\frac{1}{2}[-\lambda_2\omega_1^2\Lambda_1 + \lambda_2\omega_1\Lambda_1(2\Omega) - \lambda_2 i\omega_1^2 + \lambda_2 i\omega_1(2\Omega) + \beta_2 i + \beta_2\Lambda_1]\bar{A}_1\exp(2i\sigma T_1) \end{aligned} \tag{37}$$

and

$$\begin{cases} (\beta_1 - \omega_2^2)Q_1 - i\omega_1\omega_2\lambda_1 Q_2 = S_1 \\ -i\omega_1\omega_2\lambda_1 Q + (\beta_1 - \omega_2^2)Q_{2\ 1} = S_2 \end{cases} \tag{38}$$

where

$$\begin{aligned} S_1 &= -2i\omega_2 D_1 A_2(T_1) + \Lambda_2\lambda_1\Omega D_1 A_2 - \frac{\beta_3}{2}(6 + 2\bar{\Lambda}_1\Lambda_2 + 2\Lambda_1\bar{\Lambda}_1 + 2\Lambda_1\Lambda_2)A_1\bar{A}_1A_2 - \frac{\beta_3}{2}(3 + 2\Lambda_2\bar{\Lambda}_2 + \Lambda_2^2)A_2^2\bar{A}_2 - ic\omega_2 A_2 \\ S_2 &= -2\Lambda_2 i\omega_1 D_1 A_2 - \lambda_1\Omega D_1 A_2(T_1) - \frac{\beta_3}{2}(2\Lambda_1 + 2\Lambda_2 + 2\bar{\Lambda}_1 + 6\Lambda_1\bar{\Lambda}_1\Lambda_2)A_1\bar{A}_1A_2 - \frac{\beta_3}{2}(2\Lambda_2 + \bar{\Lambda}_2 + 3\Lambda_2^2\bar{\Lambda}_2)A_2^2\bar{A}_2 - ic\omega_2\Lambda_2 A_2 \end{aligned} \tag{39}$$

Because the coefficients matrices for Eqs.(36) and (38) are singular according to the characteristic Eq.(31), the solution do not exist unless:

$$\begin{vmatrix} (\beta_1 - \omega_1^2) & R_1 \\ i\Omega\omega_1\lambda_1 & R_2 \end{vmatrix} = 0\ ,\quad \begin{vmatrix} (\beta_1 - \omega_1^2) & S_1 \\ -i\omega_1\omega_2\lambda_1 & S_2 \end{vmatrix} = 0 \tag{40}$$

By solving the determinants of Eq. (40) and simplifying, the result will be in the form of the following equations:

$$
\begin{aligned}
&D_1A_1(T_1) = -c_2A_1^2\bar{A}_1 - c_3A_1A_2\bar{A}_2 - c_4\exp(i\sigma T_1)\ - c_5A_1 - c_6\bar{A}_1\exp(2i\sigma T_1)\\
&C_1 = (\beta_1-\omega_1^2)(+2\Lambda_1 i\omega_1 + \lambda_1\Omega) + i\omega_1^2\lambda_1(-2i\omega_1 + \lambda_1\Omega\Lambda_1)\\
&C_2 = -(\beta_1-\omega_1^2)\frac{\beta_3}{2}(2\Lambda_1 + \bar{\Lambda}_1 + 3\Lambda_1^2\bar{\Lambda}_1) + i\omega_1^2\lambda_1\frac{\beta_3}{2}(3 + 2\Lambda_1\bar{\Lambda}_1 + \Lambda_1^2)\\
&C_3 = -(\beta_1-\omega_1^2)\frac{\beta_3}{2}(2\Lambda_1 + 2\Lambda_2 + 2\bar{\Lambda}_2 + 6\Lambda_1\Lambda_2\bar{\Lambda}_2) + i\omega_1^2\lambda_1\frac{\beta_3}{2}(6 + 2\Lambda_2\bar{\Lambda}_2 + 2\Lambda_1\bar{\Lambda}_2 + 2\Lambda_1\Lambda_2)\\
&C_4 = \frac{1}{2}(\beta_1-\omega_1^2)[m_e\omega_1^2 df(l_1) + f_{mis2}f(L_2)] - \frac{1}{2}\omega_1^2\lambda_1(m_e\omega_1^2 df(l_1) + f_{mis1}f(L_2))\\
&C_5 = -(\beta_1-\omega_1^2)ic\omega_1\Lambda_1 - \omega_1^3\lambda_1 c\\
&C_6 = \frac{1}{2}[(\beta_1-\omega_1^2)(-\lambda_2\omega_1^2\Lambda_1 + \lambda_2\omega_1\Lambda_1(2\Omega) - \lambda_2 i\omega_1^2 + \lambda_2 i\omega_1(2\Omega) + \beta_2 i + \beta_2\Lambda_1) - i\omega_1^2\lambda_1(-\lambda_2\omega_1^2 + \lambda_2\omega_1(2\Omega) + \lambda_2 i\omega_1^2\Lambda_1 - \lambda_2\omega_1\Lambda_1 i(2\Omega) + \beta_2 - \beta_2 i\Lambda_1)]\\
&c_2 = -\frac{C_2}{C_1}, c_3 = -\frac{C_3}{C_1}, c_4 = -\frac{C_4}{C_1}, c_5 = -\frac{C_5}{C_1}, c_6 = -\frac{C_6}{C_1}
\end{aligned}
\tag{41}
$$

and

$$
\begin{aligned}
&D_1A_2 = -d_2A_2^2\bar{A}_2 - d_3A_1\bar{A}_1A_2 - d_4A_2\\
&D_1 = (\beta_1-\omega_2^2)(2\Lambda_2 i\omega_1 + \lambda_1\Omega) + i\omega_1\omega_2\lambda_1(2i\omega_2 - \Lambda_2\lambda_1\Omega)\\
&D_2 = -(\beta_1-\omega_2^2)\frac{\beta_3}{2}(2\Lambda_2 + \bar{\Lambda}_2 + 3\Lambda_2^2\bar{\Lambda}_2) - i\omega_1\omega_2\lambda_1\frac{\beta_3}{2}(3 + 2\Lambda_2\bar{\Lambda}_2 + \Lambda_2^2)\\
&D_3 = -(\beta_1-\omega_2^2)\frac{\beta_3}{2}(2\Lambda_1 + 2\Lambda_2 + 2\bar{\Lambda}_1 + 6\Lambda_1\bar{\Lambda}_1\Lambda_2) - i\omega_1\omega_2\lambda_1\frac{\beta_3}{2}(6 + 2\bar{\Lambda}_1\Lambda_2 + 2\Lambda_1\bar{\Lambda}_1 + 2\Lambda_1\Lambda_2)\\
&D_4 = -(\beta_1-\omega_2^2)ic\omega_2\Lambda_2 + \omega_1\omega_2^2\lambda_1 c)\\
&d_2 = -\frac{D_2}{D_1}, d_3 = -\frac{D_3}{D_1},\ d_4 = -\frac{D_4}{D_1}
\end{aligned}
\tag{42}
$$

By substitute $A_n = (1/2)(a_n\exp(i\tau_n))$ where a_n and τ_n are real constants, into Eqs.(41) and (42) and simplify them, the final solution of will be in the form of:

$$
\begin{cases}
\frac{1}{8}c_2a_1^3 + c_4\cos\Gamma + \frac{1}{2}c_5a_1 + \frac{1}{2}c_6a_1\cos 2\Gamma = 0\\
\frac{1}{2}a_1\sigma + c_4\sin\Gamma + \frac{1}{2}c_6a_1\sin 2\Gamma = 0
\end{cases}
\tag{43}
$$

where

$$
\Gamma = \sigma T_1 - \tau_1 \tag{44}
$$

In solving the equations, the value of a_2 is equal to zero. Therefore, the amount of vibration amplitude in the first resonance will be function of a_1.

In the case Ω is near the second resonance system i.e. ω_2:

Using the same process, the equations governing the system near the second resonances will be as follows:

$$
\begin{cases}
\frac{1}{8}d_2a_2^3 + d_4\cos\Gamma_2 + \frac{1}{2}d_5a_2 + \frac{1}{2}d_6a_2\sin 2\Gamma_2 = 0\\
\frac{1}{2}a_2\sigma + d_4\sin\Gamma_2 + \frac{1}{2}d_6a_2\cos 2\Gamma_2 = 0
\end{cases}
\tag{45}
$$

The Eqs. (43) and (45) in the system of equations are in terms of domain a_1 or a_2, σ; the detuning parameter and $\cos\Gamma$ or $\sin\Gamma$. According to the solution of the system of equations, $\cos\Gamma$ and $\sin\Gamma$ can be eliminated from the equations and *a* can be plotted versus σ. In Fig. 3, the vibration behavior of the rotor is shown in the first and

second resonances. As clearly indicated by the figures, resonance occurs at both critical speeds of the rotor and nonlinear terms have caused the resonance diagram form to be of a hard-spring type.

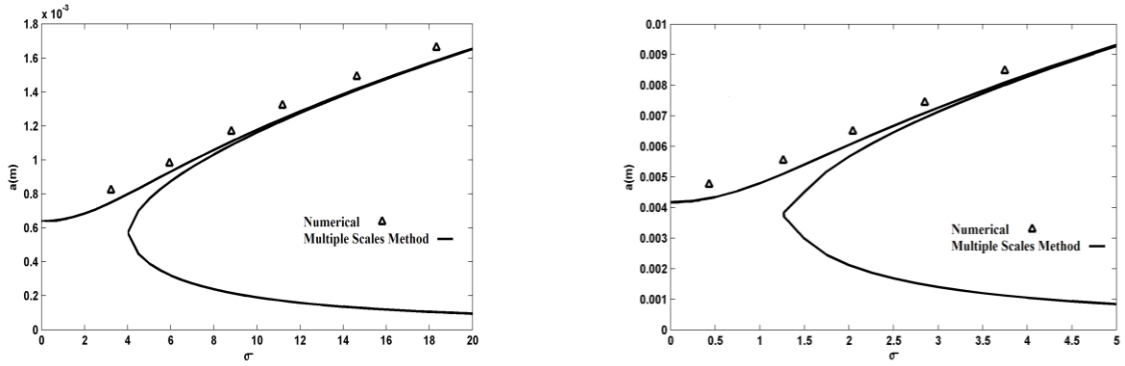

(a) (b)

Fig.3
Frequency response diagrams for the shaft with rectangular cross-section a) at the first critical speed b) second critical speed.

5 NUMERICAL STUDY

In order to examine the analytical results, a systematic analysis was conducted using the Simulink toolbox of the Matlab. The equations of motion, i.e. Eqs. (19) and (20), are directly solved by this software numerically near the first and second critical speeds and the results are shown as triangular marks in Fig.3. The numerical data are given in Appendix A4.The disadvantages of numerical methods in the analysis of non-linear problems are that unstable non-linear parts cannot be predicted, while in a multiple-scale method, these boundaries are well represented.

6 EXAMINING THE EFFECT OF SYSTEM PARAMETERS

One of the advantages of analytical methods in comparison with numerical ones is that the equations obtained are in terms of the parameters of the system and it is easy to examine the behavior of the rotor by changing its parameters. Eqs. (43) and (45) are obtained by considering the geometry of rotor, mass unbalance forces, gyroscopic effect, forces caused by misalignment and the effects of these parameters are dependent on its coefficients. The designers can change the parameters in order to predict different rotor dynamic behaviors and optimize the parameters that have the greatest effect. In this paper, simulating parameters including unbalance mass, asymmetric shaft and misalignment forces can be used to control the vibrational behavior of the system near the first and second critical speeds. In general, the effect of nonlinearity has caused the resonance curves bend from the position of the linear system response given in Appendix A3. It is interesting to note that nonlinearity due to asymmetric shaft is significantly expand the instability region in case of $\Omega = \omega_2$. The parameters' effects are discussed more in following section.

7 THE EFFECT OF THE INCREASE OF THE MASS UNBALANCE FORCE

In order to investigate the effect of unbalance mass force on the dynamic behaviors of rotor near the first and second critical speeds, the amount of unbalance mass in the disk location increased from 0.5 to 2 grams. As the magnitude of the unbalance mass increases, the amplitude of vibration is intensified and the vibration diagram inclines to the right and covers a wider range of detuning parameters, which means that the resonance at the first and second critical speeds occurs in the wider frequency range. This issue is of utmost importance in rotary machines speeds of which are higher than the critical speed, and to prevent the damage to the equipment s' passing the critical speed, the passing time should be calculated or, as far as possible, the force caused by unbalance mass should be decreased by

precise balance methods. In Fig. 4 the increase of unbalance mass force in the first and second critical speeds are shown in resonance graphs.

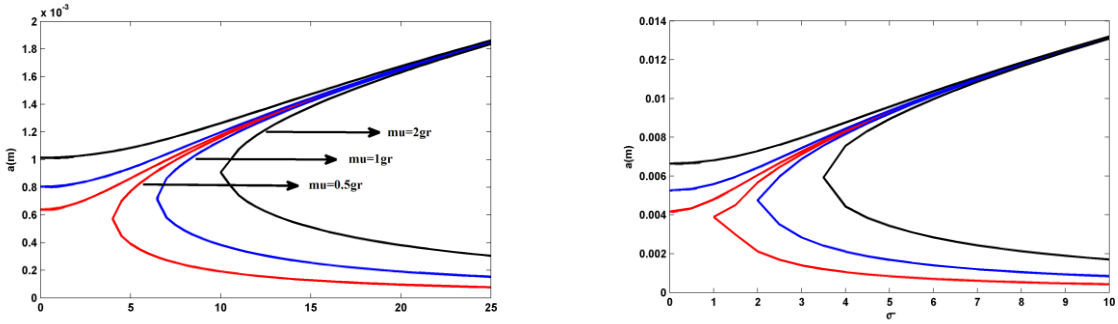

(a) (b)

Fig.4
Effect of increase in mass unbalance a) at the first critical speed b) second critical speed.

8 THE EFFECT OF INCREASING THE FORCE CAUSED BY MISALIGNMENT

As mentioned, the forces and moments caused by the unbalance force are derived from Gibbons' equations (Appendix A2). Given the fact that in the model assumed, the torque of the motor can be neglected in steady state, the effect of the forces and moments caused by the misalignment versus the transverse forces due to the misalignment can be ignored. In this paper, the magnitude of misalignment in the *z* direction is increased from 0.1 to 0.5, and its effect on the rotor's resonance curve is investigated near the first and second critical speeds, as in the case of the increase in unbalance mass, the increase of misalignment lead to the growth of the magnitude of vibration and also the frequency range of the resonance is intensified near the first and second critical speeds. In comparison with mass unbalance effect, the resonance curves are more expanded and the range of amplitude is higher. This matter is illustrated in Fig. 5.

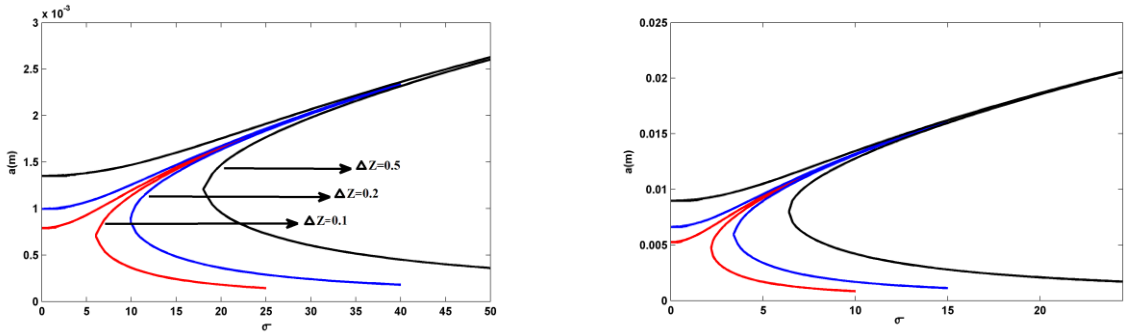

(a) (b)

Fig.5
Effect of increase in misalignment a)at the first critical speed b) second critical speed.

9 ASYMMETRIC SHAFT EFFECT

In order to investigate the effect of non-circular shaft, the length of rectangular of the cross section has been increased to twice its width. The effect of increasing the asymmetric of the shaft near the first and second critical speeds is illustrated in the rotor resonance diagram as shown in Fig. 6. The effect of changing the ratio of length to width of the cross section and, consequently, the change in the moment of inertia of the cross section near the second critical speed has led to a sharp increase in the widespread of frequency of the resonance. This means that the

effects of different parameters are not always the same on different resonances, and it is necessary to examine the effect of each of the parameters separately on the first and second resonances.

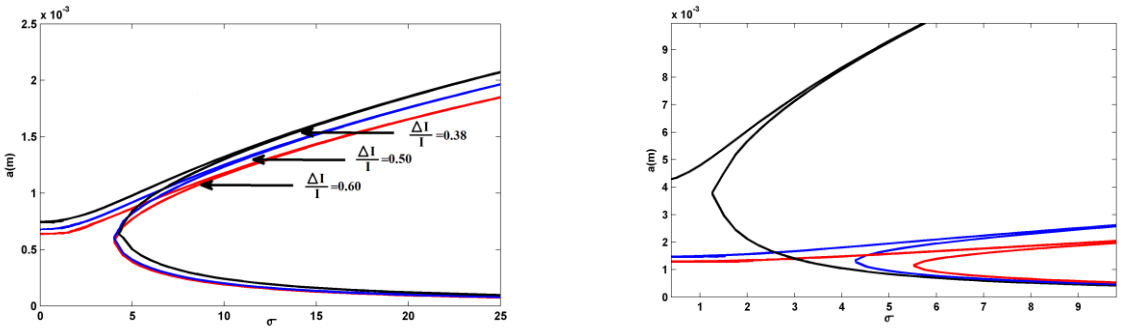

(a) (b)

Fig.6
Effect of increase in $\Delta I / I$ a) at the first critical speed b) second critical speed.

10 CONCLUSIONS

Nonlinear dynamic behavior near the primary resonances of a rotor with a rectangular shaft under the influence of forces due to coupling misalignment is investigated. Also the effects of changes in the moment of inertia of the shaft in different directions as well as gyroscopic effect are considered. Since non-linear Bernoulli theory is used for shaft modeling, nonlinear displacement effect is considered so shear force effects are neglected. To solve the equations and investigate the nonlinear behavior of the rotor, multiple scale method is used and Gibbons' equations are applied to calculate the forces due to coupling misalignment. The analytical results are verified by using numerical methods. It is observed that the analytical results are in good agreement with numerical results. As a whole, in this paper, the model of previous papers is developed. The model presented in this research is well suited to study and predict the effect of shaft asymmetry as well as other important parameters such as the effect unbalance forces, gyroscopic effect and forces caused by coupling misalignment in different speeds and especially near first and second resonances.

ACKNOWLEDGMENTS

The authors would like to thank the anonymous reviewers for their valuable and thoughtful comments to improve the quality of this work.

APPENDIX

A.1 Nomenclature

a_1	Amplitude at the equilibrium position (m) in x direction
a_2	Amplitude at the equilibrium position (m) in z direction
Ω	Angular Speed of rotor ($rad\ sec^{-1}$)
ω_1, ω_2	Angular frequencies of rotor ($rad\ sec^{-1}$)
I	Area moment of inertia of shaft (m^4)
c	Coefficient of damping ($N\ s\ m^{-1}$)
R_1	Cross sectional radius of shaft/internal radius of disk (m^2)
A	Cross sectional area of shaft (m^2)
q	Density of material ($kg\ m^{-3}$)
r_1	Detuning parameter ($rad\ sec^{-1}$)
U	Discretized displacement along axis x (m)

W Discretized displacement along axis z (m)
$u(y,t)$ Displacement along x axis of rotor (m)
$w(y,t)$ Displacement along z axis of rotor (m)
T_s Kinetic energy of shaft ($N\,m$)
T_D Kinetic energy of disk ($N\,m$)
T_u Kinetic energy of mass unbalance ($N\,m$)
L Length of shaft (m)
I_{dx} Mass moment of inertia of disk in direction x ($kg\,m^2$)
I_{dv} Mass moment of inertia of disk in direction y ($kg\,m^2$)
M_d Mass of disk (kg)
d_1 Position of mass unbalance from geometric center of shaft (m)
l_1 Position of disk on shaft (m)
U_s Strain (deformation) energy of shaft ($N\,m$)
h Thickness of disk (m)
T_R Total kinetic energy of rotor ($N\,m$)
U_R Total strain (deformation) energy of rotor ($N\,m$)

A.2 Misalignment reaction forces and moments

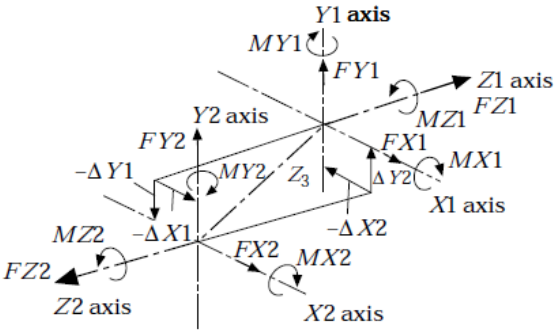

Fig.A.2
Coupling coordinates system.

$$\begin{cases} MX\,1 = Tq\sin\theta_1 + K_b\phi_1 & , MX\,2 = Tq\sin\theta_2 - K_b\phi_2 \\ MY\,1 = Tq\sin\phi_1 - K_b\theta_1 & , MY\,2 = Tq\sin\phi_2 + K_b\theta_2 \\ MZ\,1 = Tq & , MZ\,2 = -Tq \\ FX\,1 = (-MY\,1 - MY\,2)/Z\,3 & , FX\,2 = -FX\,1 \\ FY\,1 = (MX\,1 + MX\,2)/Z\,3 & , FY\,2 = -FY\,1 \end{cases} \quad \text{(A.2a)}$$

where

$$\begin{cases} \theta_1 = Arc\sin(\Delta X1/Z3) & , \theta_2 = Arc\sin(\Delta X2/Z3) \\ \phi_1 = Arc\sin(\Delta Y1/Z3) & , \phi_2 = Arc\sin(\Delta Y2/Z3) \end{cases} \quad \text{(A.2b)}$$

A.3 Linear analysis

The rotor is analyzed as a free un-damped linear system to determine natural frequencies and in Fig. A.3(a) Campbell diagram is plotted to determine the rotor critical speeds. Two critical speeds are found to be 1096.5 *rpm* and 1148.7 *rpm*. The unbalanced mass response is also shown in Fig. A.3(b).

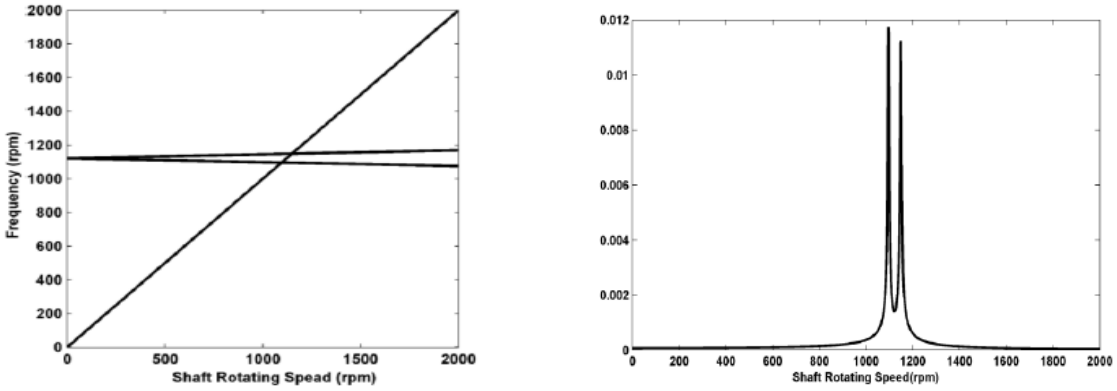

(a) (b)

Fig.A.3
a) Campbell diagram. b) Mass unbalance response.

A.4 Numerical data

Geometric and material property:

$$\rho = 7800 kgm^{-3}, \quad E = 200\times 10^{9}\, Nm^{-2} \quad , c = 0.001$$

$$Shaft: \ L_1 = 92mm, \ L = 0.24, \quad L = 320, \ Sx = 4mm, Sz = 6mm(rec\tan gular\ cross\ \sec tion\ 4\times 6)$$

$$Disk: \quad M_D = 1.561Kg, \quad R_1 = 19mm \ , R_2 = 150mm \ , h = 10mm, \ I_{Dx} = M_D(3R_1^2 + 3R_2^2 + h^2)/12$$

$$I_{Dy} = M_D(R_1^2 + R_2^2)/2$$

Constant

$$\lambda_1 = 0.046, \lambda_2 = 3.3582\times 10^{-6}, \beta_1 = 1.3788\times 10^{4}, \beta_2 = 5.3032\times 10^{3}, \beta_3 = 4.7729\times 10^{9}$$

REFERENCES

[1] Tondl A., 1965, *Some Problems of Rotor Dynamics*, Publishing House of the Czechoslovak Academy of Sciences, Prague.

[2] Badlani M., Kleinhenz W., 1978, The effect of rotary inertia and shear deformation on the parametric stability of unsymmetric shafts, *Mechanism and Mashine Theory* **13**: 543-553.

[3] Sheu H.-C., Chen L.-W., 2000, A lumped mass model for parametric instability analysis of cantilever shaft-disk systems, *Journal of Sound and Vibration* **234**: 331-348.

[4] Pei Y.-C., 2009, Stability boundaries of a spinning rotor with parametrically excited gyroscopic system, *European Journal of Mechanics - A/Solids* **28**: 891-896.

[5] Shahgholi M., Khadem S.E., 2012, Primary and parametric resonances of asymmetrical rotating shafts with stretching nonlinearity, *Mechanism and Machine Theory* **51**: 131-144.

[6] Jafari A.A., Jamshidi P., 2015, Investigating the stability of rotors with asymmetry cross sections using perturbation method, *The 5th International Conference on Acoustics and Vibrations*.

[7] Gibbons C., 1976, Coupling misalignment forces, *Proceedings 5th Turbomachinery Symposium, Turbomachinery Laboratory*, Texas A&M University, College Station, Texas.

[8] Sekhar A., Prabu B., 1995, Effects of coupling misalignment on vibrations of rotating machinery, *Journal of Sound and Vibration* **185**(4): 655-671.

[9] Al-Hussain K.M., Redmond I., 2002, Dynamic response of two rotors connected by rigid mechanical coupling with parallel misalignment, *Journal of Sound and Vibration* **249**(3): 483-498.

[10] Al-Hussain K.M., 2003, Dynamic stability of two rigid rotors connected by a flexible coupling with angular misalignment, *Journal of Sound and Vibration* **266**(2): 217-234

[11] Lees A. W., 2007, Misalignment in rigidly coupled rotors, *Journal of Sound and Vibration* **305**: 261-271.

[12] Patel T.H., Darpe A.K., 2009, Experimental investigations on vibration response of misaligned rotors, *Mechanical Systems and Signal Processing* **23**(7): 2236-2252.
[13] Patel T.H., Darpe A.K., 2009, Vibration response of misaligned rotors, *Journal of Sound and Vibration* **325**(3): 609-628
[14] Pennacchi P., Vania A. , Chatterton S., 2012, Nonlinear effect caused by coupling misalignment in rotors equipped with journal bearing, *Mechanical and Systems and Signal Processing* **30**: 306-322.
[15] Ma H., Wang X., Niu N., Wen B., 2015, Oil-film instability simulation in an overhung rotor system with flexible coupling misalignment, *Archive of Applied Mechanics* **85**: 893-907.
[16] Feng S., Geng H., Qi S., Yu L., 2012, Vibration of a misaligned rotor system with asymmetric shaft stiffness, *Advanced Materials Research* **503-504**: 813-818.
[17] Lalanne M., Ferraris G., 1998, *Rotordynamics Prediction in Engineering*, John Wiley & Sons.
[18] Kr.Jalan A., Mohanty A.R., 2009, Modal based fault diagnosis of a rotor-bearing system for misalignment and unbalance under steady-state condition, *Journal of Sound and Vibration* **327**: 604-622.
[19] Nayfeh A.H., Mook D.T., 1979, *Nonlinear Oscillations*, Wiley, New York.